A study on stress corrosion cracking of fine grain steel

Proceedings of the Sixteenth (2006) International Offshore and Polar Engineering Conference
San Francisco, California, USA, May 28-June 2, 2006

ISBN 1-880653-66-4 (Set); ISSN 1098-6189 (Set)

A Study on Stress Corrosion Cracking of Fine Grain Steel

Zhijian Huang
Graduate school of Natural Science and Technology, Kanazawa University
Kanazawa, Ishikawa , Japan

Masahide Gotoh
Venture Business Laboratory, Kanazawa University
Kanazawa, Ishikawa, Japan

Masayuki Shozu
Maizuru National College of Technology
Maizuru, kyoto, Japan

Yukio Hirose
Department of Materials Science and Engineering, Kanazawa University
Kanazawa, Ishikawa, Japan

ABSTRACT

It is known that fine grain steel possesses high strength according to Hall-Petch relation and therefor many researchers are examining to use the fine grain steel on civil engineering and architecture fields as next generation's high strength material. Then the evaluation of corrosion resistance property to fine grain steel is very important.

In this study, Stress Corrosion Cracking test was done on specimens of the fine grain steel and conventional steel. Afterwards fracture surfaces were observed with SEM (Scanning Electron Microscope) and the residual stresses under the fracture surfaces were measured by X-ray stress measurement. The difference of stress corrosion resistance property between fine grain steel and conventional steel was clarified.

KEY WORDS: Fine grain steel; Stress Corrosion; X-ray; SEM fractography; Residual stress; NFG600; SM490.

INTRODUCTION

Steel is a vital material for industry and the mechanical and functional properties expected of steel material are increasing with the development of industrial technology. Social factors such as a move towards energy and saving resource and environment conservation mean that the demand for lighter and more recyclable steel materials is also growing. Recently it has become clear from the results of basic research that properties such as strength, toughness can be improved by reducing grain size. In other words, fine grain steel is a steel material which possesses higher strength and longevity than conventional steel. Fine grained microstructure is attained by High Reduction Rolling and Strong Cooling. The chemical compositions of the fine grain steel are almost same with conventional steel, but the grain size is different. Fine grain steel not only has improved strength, but also has superior formability and weldability. So it will be used on many fields as next generation's high strength material. In this case, it is necessary to realize the strength characteristic and environmental characteristic of fine grain steel under corrosion environment. Otherwise, it is important to understand the mechanism of the crack growth and the remaining longevity of the material to realize the growth behavior of the crack occurred by stress corrosion cracking.

The purpose of this study is to clarify the influence on stress corrosion resistance property of the crystal grain size via Stress Corrosion Cracking (SCC) test, SEM (Scanning Electron Microscope) fractography and residual stress analysis with X-ray stress measurement on specimens of the fine grain steel and conventional steel.

EXPERIMENTAL METHOD

Materials and Specimens

SM490 (conventional rolling steel) and NFG600 (fine grain steel) were used in this study. NFG600 is a SM490 material whose ferrite grain size was reduced. So NFG600 has same chemical compositions as SM490, but has different ferrite grain size. Fig.1 shows microstructures of NFG600 and SM490. RD is the rolling direction. The ferrite grain diameter of NFG600 is 2-5μm and the ferrite grain diameter of SM490 is 10-15μm. The ferrite grain size of NFG600 is about 1/3 smaller compared to SM490. Table 1, 2 show chemical compositions and mechanical properties of NFG600 and SM490.

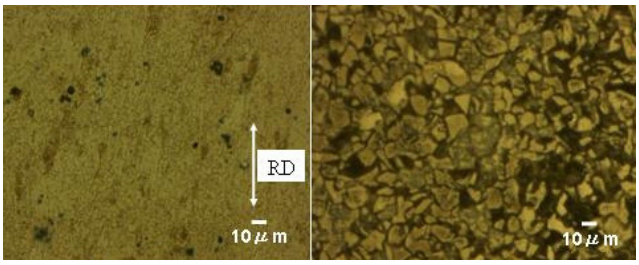

(a) NFG600, grain diameter≈5μm (b) SM490, grain diameter≈15μm
Fig.1 Microstructures of NFG600 and SM490

Table 1 Chemical compositions (wt. %)

	C	Si	Mn	P	S
NFG600	0.16	0.40	1.40	0.010	0.005
SM490	0.16	0.40	1.40	0.010	0.005

Table 2 Mechanical properties

	Yield stress σ_Y, MPa	Tensile strength σ_B, MPa	Elongation ε_1, %	Vickers Hardness HV
NFG600	422	555	26	183
SM490	341	500	29	166

Specimens of NFG600 and SM490 were prepared by milling processing and grinding processing. Every specimen has dimensions of 100×20×10 mm^3. After shape processing, a notch whose length was 10 mm was cut by wire cutter at every specimen and the curvature radius of the notch ρ is 0.18 mm. At last, the influence of residual stress that generated in the mechanical processing was eliminated by electrochemical-polishing. Then it is confirmed that the value of residual stress generated by SCC test which is obtained via X-ray stress measurement is reliable. Fig.2 shows dimensions of specimen.

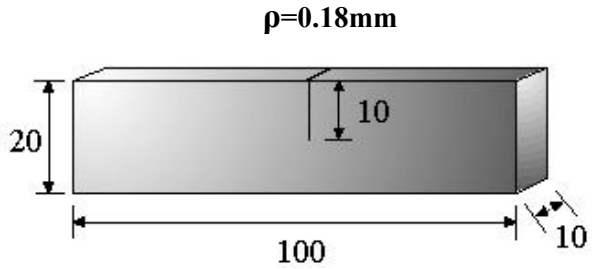

Fig.2 Dimensions of specimen

Stress Corrosion Cracking test

The objective of this test is to examine the influence on crack nucleation time etc. by difference of crystal grain diameter. The schematic illustration of Stress Corrosion Cracking test is shown in Fig.3. The corrosive liquid was 3.5% NaCl aq. The load is generated by tightening the bolt, and the load is given to the specimen by the reaction force. The crack opening displacement in the notch is measured with the clip gauge. The strain gauge measures the load which is given to the specimen. In this study, a constant load which was within the range of 850kg-1000kg was given to the specimen and kept until the crack was generated. It was confirmed to have caused the crack in specimen by the crack opening displacement of the clip gauge. The specimen was soaked in the NaCl liquid for five minutes after the crack was caused, then was taken out the solution and fractured by using hammer. In this study, it was scheduled that same experiments are done by taking ρ=0, ρ=0.18 mm, ρ=0.40 mm etc respectively, but the current, the experiments were done only by taking ρ=0.18 mm. Eq.1 is an equation for stress intensity of an infinitely sharp crack (ρ=0). K_ρ is apparent stress intensity factor in which ρ is assumed to be a parameter. In the original research of the SCC crack, the influence of ρ was discussed. (Hirose, Yajima and Tanaka, 1983) Apparent stress intensity factor, K_ρ, for blunt notches was calculated by assuming ρ=0, then it is expressed as Eq.1. Where, S is the span between point a and point b in Fig.3, P is the load, a is the crack length which include the SCC crack length, W is the specimen height and t is the specimen thickness. According to Eq.1, the value of apparent stress intensity factor K_ρ was calculated from the load and the crack length.

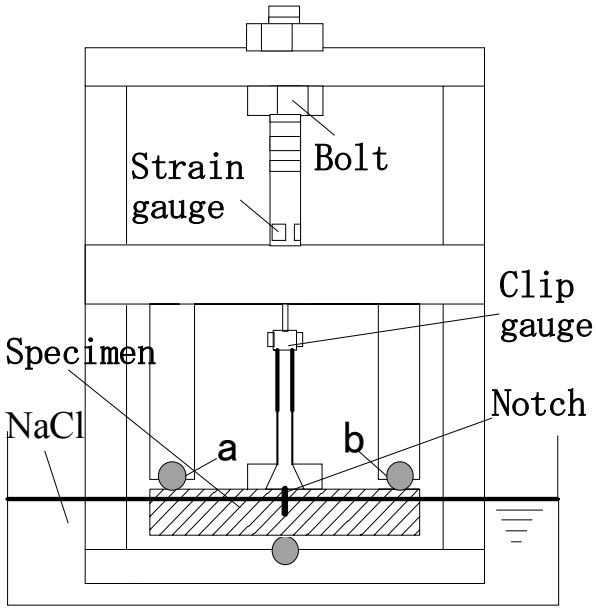

Fig.3 Stress Corrosion Cracking test equipment

$$K_\rho = \frac{3SP}{2Wt^2}\sqrt{\pi a}\,F(a/W) \quad (1)$$

SEM Fractography

After Stress Corrosion Cracking, fracture surfaces on specimens were observed with SEM (Scanning Electron Microscope). The objective of observing fracture surface is to confirm the fracture mode of the specimens and the position of the crack. The SEM equipment used for observation was HITACHI S-4500 FE-SEM. The samples were broken open during the SCC test and the main observation position was the starting point of the crack.

Residual stress analysis with X-ray stress measurement

After the SCC test, residual stresses were measured by X-ray stress

measurement method. Optical layout of X-ray measurement system is shown in Fig.4, and measurement conditions are listed in Table 3. Residual stress is obtained from a gradient of straight-line obtained from $\sin^2\psi$ diagram. The $\sin^2\psi$ diagram is drawn by measurement of Bragg angle 2θ every tilt angle ψ. In biaxial stress state, the stress σ_x can be expressed as

$$\sigma_x = K \cdot M \quad \text{[MPa]} \tag{2}$$

$$K = -\frac{E}{2(1+\nu)} \cdot \cot\theta_0 \cdot \frac{\pi}{180} \quad \text{[MPa/deg]} \tag{3}$$

$$M = \frac{\partial(2\theta)}{\partial(\sin^2\psi)} \quad \text{[deg]} \tag{4}$$

where, M is a gradient of straight-line obtained from $\sin^2\psi$ diagram. K is stress constant. E is X-ray Young's modulus, and ν is called X-ray Poisson's ratio. E and ν depend on the diffraction plane. θ_0 is a diffraction angle with free stress state.

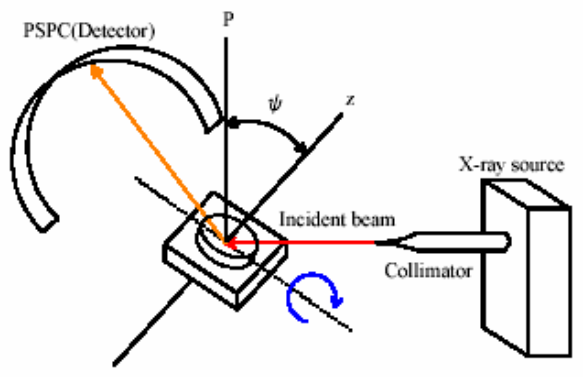

Fig.4 Schematic illustration of X-ray optical system

Table 3 Conditions for X-ray stress measurement

Characteristic X-ray	Cr-Kα
Diffraction plane	Fe211
Filter	V foil
Tube voltage	30kV
Tube current	60mA
Scanning method	Iso inclination

The residual stress measurements were conducted after the SCC test. The purpose of residual stresses measurement after the SCC test is to obtain the plastic zone size from the residual stresses distribution in the depth direction. The plastic zone size ω_y is defined as the distance at which the residual stress approaches to the initial value.

In fracture mechanics, plastic zone size ω_y can be expressed as

$$\omega_y = \alpha\left(\frac{K}{\sigma_y}\right)^2 \tag{5}$$

Eq.5 is an equation which shows the plastic zone size of a vertical direction to the crack. where, K is the stress intensity factor, σ_y is yield stress and α is peculiar constant value of material. In this study, ω_y was obtained from the tests of measuring residual stress, σ_y is constant value and was obtained from tensile test, K was calculated from Eq.1, so α can be calculated from Eq.5.

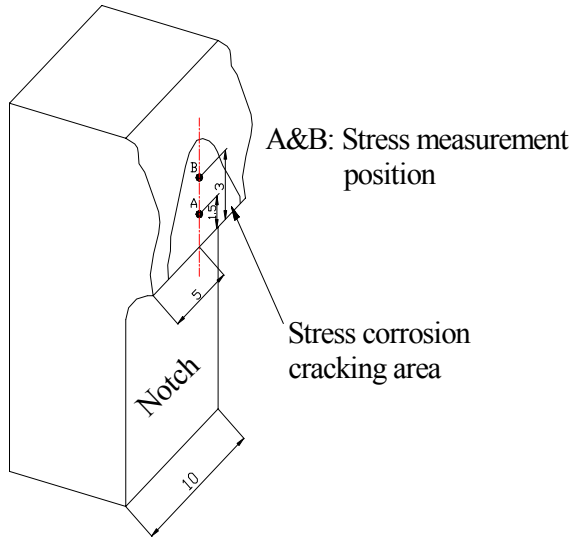

Fig.5 Measurement position of X-ray stress analysis

Two stress measurement positions were selected for the comparison. Fig.5 shows the location of stress measurement. Point A and point B located in stress corrosion cracking area were locations of stress measurement. The distance from the centre of notch bottom to point A is 1.5mm and the one from the centre of notch bottom to point B is 3mm. The distribution of residual stresses in the direction of the depth was obtained by irradiating X-ray on the new surface revealed by successive electro-polishing using 85%H_3PO_4. Residual stresses were measured every 10 μm thickness until the residual stresses from the Stress Corrosion Cracking test disappear.

EXPERIMENTAL RESULTS AND DISCCUSION

Results of Stress Corrosion Cracking test

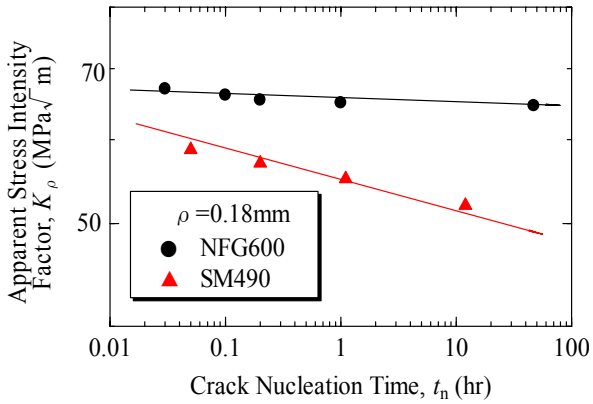

Fig.6 Relationship between $K\rho$ and t_n

Fig.6 shows the relationship between crack nucleation time and apparent stress intensity factor which was obtained from SCC test. As shown in the figure, the inclination of the graph of NFG600 is more gradual, so NFG600 is shown to have better stress corrosion cracking resistance than SM490 as measured by this test. Otherwise, it is a possibility that crack nucleation time can be forecast from the straight line.

Results of SEM fractography

(a) SEM observation position of NFG600

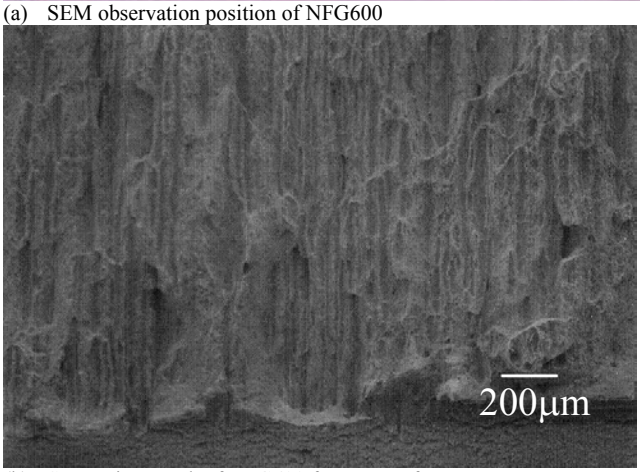

(b) SEM micrograph of NFG600 fracture surface

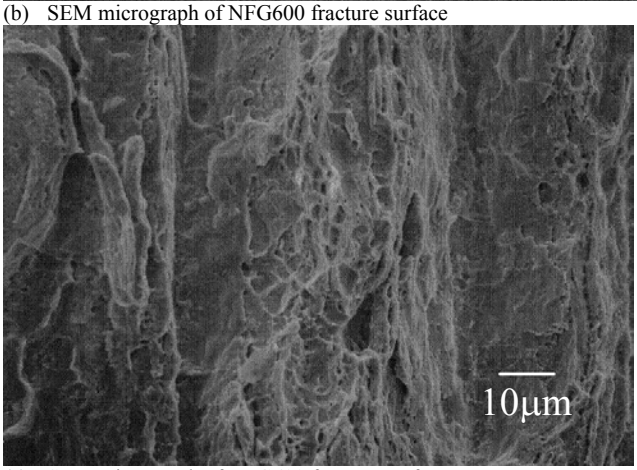

(c) SEM micrograph of NFG600 fracture surface

Fig.7 SEM fractography of NFG600

(a) SEM observation position of SM490

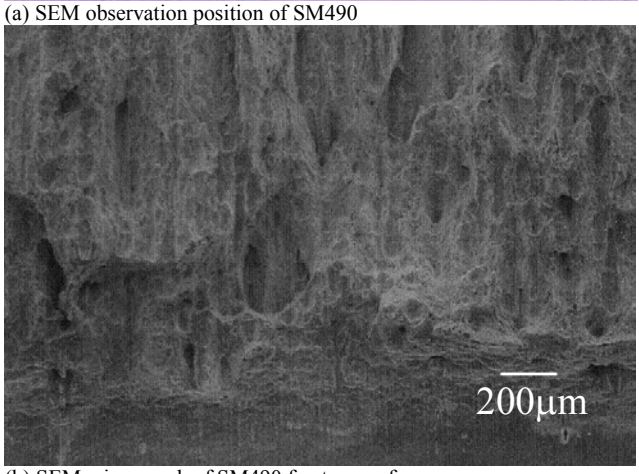

(b) SEM micrograph of SM490 fracture surface

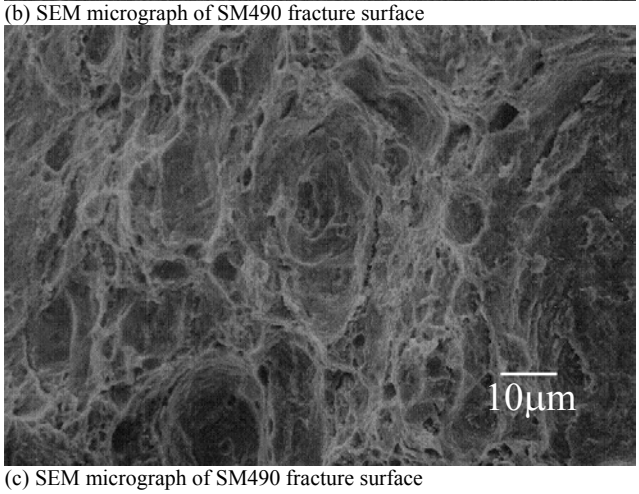

(c) SEM micrograph of SM490 fracture surface

Fig.8 SEM fractography of SM490

SEM micrograph of NFG600 fracture surface is shown in Fig.7 and SEM micrograph of SM490 fracture surface is shown in Fig.8. From all SEM micrographs of NFG600 and SM490, the coexistence of fracture ductility and the form of embrittlement could be seen. The characteristic of fracture ductility is dimple rupture which usually occurs under single load or tearing. Stress-corrosion cracking was identified as intergranular and transgranular cracks which reveals the form of embrittlement due to interaction between the stresses and the corrosive environment. Otherwise, the amount of dimple in NFG600

fracture surface is less than that of SM490 fracture surface, so it was thought that SM490 causes the fracture ductility easily than NFG600. Moreover, because the crack size of SM490 whose grain size is larger than that of NFG600, it is possible that the crack size is related to the grain size of the material.

NFG600 and SM490 are both the material which shows ductility comparatively behavior. However, according to the destruction style of the stress corrosion cracking, it was thought that embrittlement damage was caused firstly, and the stress concentration on the crack point was generated after the crack growth stopped, then the coexistence of fracture ductility and the form of embrittlement was formed by the repetitions of above processes.

Results of residual stress analysis using X-ray

Fig.9 shows the distribution of residual stresses in the depth direction measured on the position A and B of NFG600 fracture surface. During the SCC test, the plastic deformation was caused along with the crack generation and the residual stresses were formed by the plastic deformation. Moreover, the initial residual stresses were also generated by base metal processing. So the residual stress values measured by X-ray include the residual stresses from SCC test and from base metal processing, then the settled point of the residual stress values is not 0. In the diagram of residual stresses distribution on the depth direction, the plastic zone size ω_y is the depth range which is from 0μm to the settled point of the residual stress value. So from Fig.9, ω_y of stress measurement position A and B are about 100 μm and 280 μm respectively. In other word, the further the distance from the notch bottom is, the larger the plastic zone size ω_y is.

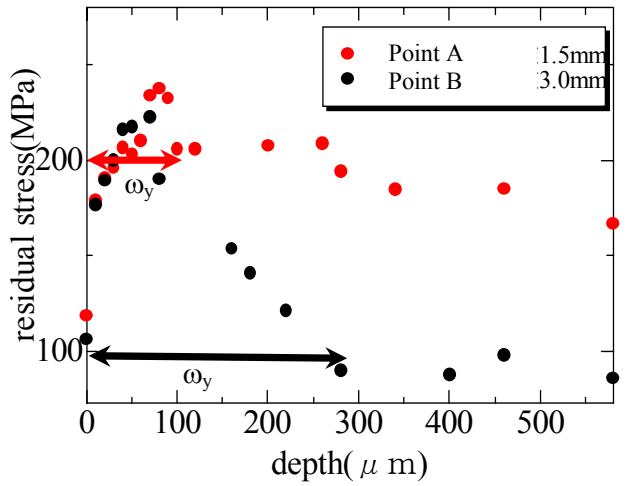

Fig.9 Residual stresses distribution in the depth direction of NFG600

As shown in Fig.9, the residual stresses under the NFG600 fracture surface were tensile stresses. The residual stress distribution rises at first, then descends. The cause is that residual stress opening happened because the crack was caused.

Otherwise, Eq.6 was obtained from Eq.5,

$$\log w_y = 2\log\alpha + 2\log(\frac{K}{\sigma_y}) \quad (6)$$

According to Eq.6, ω_y should be linear with K/σ_y. K/σ_y is the fracture mechanics parameter. Fig.10 shows the relation between fracture mechanics parameter K/σ_y and ω_y of NFG600. The line is the theory approximate line whose gradient is 2 obtained from Eq.6. The peculiar constant α is obtained from Eq.6 and Fig.10, and α=0.00298, this value is smaller than the one α=π/3 which exists in the report of the past.

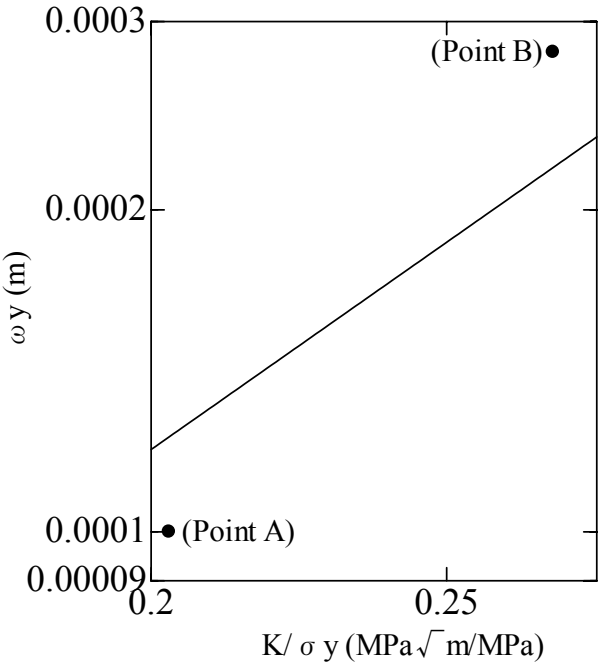

Fig.10 Relation between fracture mechanics parameter and ω_y (NFG)

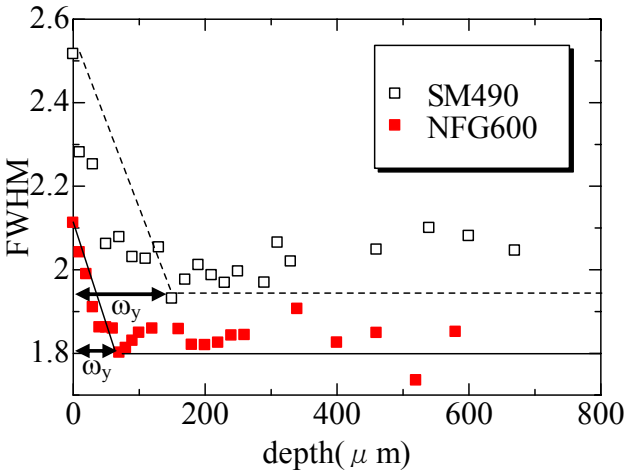

Fig.11 FWHM distribution in the depth direction

Fig.11 shows the difference between NFG600 and SM490 in the FWHM distribution. The technical term Full-Width Half-Maximum, or FWHM, is used to describe a measurement of the width of an object in

a picture, when that object does not have sharp edges. The plastic zone size ω_y is obtained from FWHM distribution in the depth direction. As shown in Fig.11, ω_y of NFG600 is smaller than that of SM490. The cause is that NFG600 has stronger yield strength because of the smaller grain size.

CONCLUSIONS

It was clarified that the influence on stress corrosion resistance property of the grain size by using NFG600 and SM490. The main results obtained in this study are summarized as follows:

(1) Fine grain steel NFG600 is shown to have better stress corrosion cracking resistance than SM490 as measured by Stress Corrosion Cracking test.

(2) On both NFG600 fracture surface and SM490 fracture surface, the coexistence of fracture ductility and the form of embrittlement is formed. However, SM490 causes the fracture ductility more easily than NFG600. Otherwise, maybe the crack size is related to the grain size of the material.

(3) The difference of plastic zone size ω_y due to the difference of the crystal grain size was confirmed. ω_y of NFG600 is smaller than ω_y of SM490 because fine grain steel NFG600 has stronger yield strength.

ACKNOWLEDGEMENTS

Thank Mr. Lei Che (Kanazawa University) and Mr. Kenichiro Suzuki (Kanazawa University) for their support of this work.

REFERENCES

Hagiwara, Y and Suzuki, H (2000) “Fracture mechanics (in Japanese)” Ohmsha Publishing Company, ISBN 4-274-13201-3.

Hirose, Y, Yajima Z, Tanaka K (1983) “X-ray Fractography on Stress Corrosion Cracking of High Strength Steel”, Advances in X-ray Analysis, Vol 27, pp.213-220

Tanaka, K and Hirose, Y (1988) “X-ray fractography (in Japanese)”, The Society of Materials Science, Japan, Vol 37, No421, pp.112-123

Huang, ZJ, Gotoh, M, Shozu, M and Hirose, Y (2005). “Residual Stress Generated by Grinding of Fine Grain Rolling Steel”, *Proceedings of The Fifteenth International Offshore and Polar Engineering Conference*, pp.218-223.

Rice JR(1977). “Mechanics of Crack Tip Deformation and Extension by Fatigue”, *Fatigue Crack Propagation, ASTM STP 415*, Am. Soc. Testing Mats., pp.247-306.

The Society of Materials Science, Japan (2002). “Standard of X-ray stress measurement (in Japanese)”, JSMS Committee on X-ray Study of Mechanical Behavior of Materials. ISBN 4-901381-14-8.

Nakasono, S, Nakamura, K, Sode, K and Matsunaga, T (1992). “Electrochemical disinfection of marine bacteria attached on a plastic electrode”, Bioelectrochemistry and Bioenergetics; A Section of Journal of Electroanal. Chem., and constituting, Vol 342, No27, pp.191-198

Cullity, BD (1977). “Elements of X-ray diffraction” Addison-Wesley Publishing Company, Inc. ISBN 0-201-01174-3.

Noyan, IC, Cohen, JB. (1987). “Residual Stress Measurement by Diffraction and Interpretation”, Springer-Verlag New York Inc. ISBN 0-387-96378-2.

The Society of Materials Science, Japan (1981). “X-ray stress measurement (in Japanese)”, yokendo co.ltd. ISBN 4842501057.